Archives of Acoustics Vol. 51, No. 2, pp. 415–426 (2026), https://doi.org/10.24423/archacoust.2026.4332

OSA 2025

Impact of Perforated Sheet Geometry on the Insertion Loss of Absorptive Silencers

Kamil Wójciak*, Joanna Maria Kopania, Patryk Gaj

Institute of Power Engineering – National Research Institute
Warsaw, Poland

*Corresponding Author: kamil.wojciak@itc.edu.pl

Received September 12, 2025; revised December 15, 2025; accepted March 18, 2026; available online March 26, 2026; version of record June 3, 2026; published issue June 24, 2026.

This study evaluates the influence of perforated sheet geometry on the acoustic and aerodynamic performance of absorptive silencers. A modular silencer is developed, enabling the installation of six different perforated metal sheets with varying hole shapes (round, square, elongated), sizes (2 mm to 20 mm), and open area ratios (22 % to 45 %). Glass wool is used as the sound-absorbing filling. Insertion loss, self-noise, and pressure drop are measured in a large reverberation chamber, within the frequency range from 50 Hz to 10 000 Hz, for airflow velocities of 4 m/s, 6 m/s, and 8 m/s. The results indicate that all configurations provide comparable attenuation at low frequencies. Silencers with small round perforations (diameter 2 mm to 6 mm) ensure higher insertion loss and lower self-noise in the mid-frequency range of 1000 Hz to 5000 Hz, without any measurable increase in pressure drop compared to variants with larger or elongated holes. For frequencies above 6300 Hz, perforated sheets with larger holes perform better. Pressure loss differences between all configurations do not exceed 1 Pa at a given flow velocity. The results confirm that aperture size is the primary parameter affecting silencer acoustic effectiveness, while aperture shape and perforation ratio are secondary. These findings provide practical guidelines for optimal silencer design in ventilation systems, ensuring maximum noise reduction with minimal airflow resistance.

Keywords: silencers, insertion loss, experimental test, aeroacoustics, ventilation.

Notations

D_i – insertion loss,
L_W – sound power level,
L_{WI} – sound power level with the test object installed,
L_{WII} – sound power level with the substitution element replacing the test object,
v – flow velocity,
Δp – pressure loss.

1. Introduction

Noise generated by mechanical ventilation systems has become a significant challenge in residential buildings, directly affecting occupant comfort and sleep quality (Harvie-Clark *et al.*, 2019; Abramkina, 2023). Excessive sound levels often lead residents to disable or reduce the use of ventilation, resulting in poor indoor air quality and potential health risks, especially in modern airtight dwellings (Harvie-Clark *et al.*, 2019; Lan *et al.*, 2021). Studies confirm that, while adequate ventilation is essential for maintaining healthy living conditions and improving sleep, these benefits are only realised if ventilation noise is kept to a minimum (Lan *et al.*, 2021). Furthermore, official standards and guideline values for acceptable noise levels in living spaces vary across countries, but recent

recommendations highlight the need to maintain bedroom noise levels below 30 dB(A) to prevent adverse effects on sleep and well-being (Harvie-Clark *et al.*, 2019). Noise in ventilation systems originates from multiple sources such as fans, dampers, control devices, and turbulent airflow, and the overall perceived noise is often exacerbated by improper design or installation (Abramkina, 2023). Consequently, the application of effective acoustic silencers within ventilation systems is crucial for reducing noise emissions, as demonstrated by both engineering analyses and practical experience (Abramkina, 2023).

Perforated metal sheets are widely used as interface elements in absorptive silencers to separate the sound-absorbing material from the duct interior while permitting airflow. The acoustic performance of such silencers is influenced by the properties of the perforated panel, including perforation geometry, open area ratio, and the physical dimensions of both the panel and the absorber. Previous studies have primarily focused on micro-perforated panels (MPPs), where sub-millimetre holes provide the necessary acoustic resistance to achieve broadband sound absorption without the use of porous materials (Maa, 1998; Wu, 1997). The theoretical basis for MPPs, as outlined by Maa (1998), models the holes as arrays of short tubes, characterising the system in terms of acoustic impedance, porosity, and perforation constant, which collectively determine the absorption bandwidth and resonance frequency. MPPs have been implemented in a range of noise control applications, such as room acoustics (Kang, Brocklesby, 2005; Hoshi *et al.*, 2020), ventilation systems (Yu *et al.*, 2016; Zhang *et al.*, 2020; Wójciak *et al.*, 2025), and transparent noise barriers (Asdrubali, Pispola, 2007).

Despite the extensive literature on micro-perforated solutions, the majority of these studies are limited to circular holes with diameters below 1 mm, and relatively little attention has been paid to panels with larger or non-circular perforations in silencer configurations. Classic MPP models do not account for the flow and acoustic effects associated with larger-scale or differently shaped openings. In practice, many industrial silencers use panels with millimetre-scale and non-circular perforations, where the contribution to both acoustic attenuation and flow characteristics may differ fundamentally from micro-perforated designs (Wu, 1997; Allam, Ĺbom, 2011).

The acoustic interaction between the perforated sheet, the porous absorber, and the silencer geometry is also affected by backing cavity configuration, flow presence, and the spatial coupling of acoustic modes (Yang *et al.*, 2015; Yang, Cheng, 2016). For typical absorptive silencers utilising porous materials, increasing the open area ratio and altering perforation geometry modify the sound transmission and pressure loss characteristics, as well as the generation of self-noise (Maa, 1998). However, the impact of non-micro-perforated panels (particularly those with varying hole shapes) on silencer efficiency, self-generated noise, and flow resistance has seldom been assessed.

Acoustic silencers play a pivotal role in reducing ventilation noise, and their design and selection must be tailored to the specific acoustic requirements and airflow conditions of each system. However, there is a lack of comprehensive data on how perforated sheet geometry in absorptive silencers affects noise attenuation, self-noise, and pressure loss. The present study investigates the effect of perforated metal sheets with different hole sizes and geometries, beyond the micro-perforation range, on the effectiveness of absorptive silencers. Using a modular silencer test rig with interchangeable side panels, the study enables direct comparison of circular, square, and elongated perforations with different open area ratios. Measurements were performed in accordance with ISO 7235 (International Organization for Standardization [ISO], 2003), using glass wool as the absorptive filling, and insertion loss was evaluated over a broad frequency range in third-octave bands. The outcomes provide insight into the relationship between perforated sheet parameters and silencer performance under practical conditions, contributing to the optimisation of silencer design in industrial applications.

2. Test objects

The subject of the investigation is an absorptive silencer designed to assess the influence of perforated sheet properties on insertion loss, flow noise and pressure loss. In this configuration, the perforated sheet is utilised as a partition between the airflow channel within the silencer and the adjacent layer of sound-absorbing material. The silencer features a modular construction, comprising an outer casing equipped with two interchangeable side panels, thus enabling the installation of panels with a maximum thickness of 300 mm. The remaining two sides

of the enclosure are fabricated from 3 mm-thick steel sheet, providing mechanical rigidity and acoustic isolation. The 3D model of the silencer constructed for measurements is presented in Fig. 1.

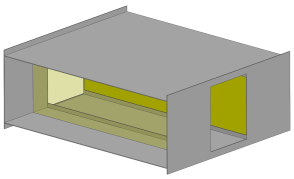

FIG. 1. 3D model of the silencer constructed for measurements.

The silencer is fitted with a rectangular connecting flange having internal dimensions of 315 mm by 250 mm. The total length of the silencer, measured between the inlet and outlet connections, is 1000 mm. The replaceable side panels have dimensions of 320 mm by 1000 mm, allowing for direct comparison of the acoustic effectiveness of various perforated sheets and reference materials. The principal dimensions of the silencer are shown in Fig. 2. The sound-absorbing material selected for the study is Ventilux 6335 glass wool, with a thickness of 100 mm and a density of 35 kg/m^3 (GAJ *et al.*, 2019), which is positioned directly behind the perforated sheet along the airflow path. The same set of glass wool slabs is used for all perforated-sheet variants and all measurement series, ensuring identical acoustic filling conditions for each test configuration.

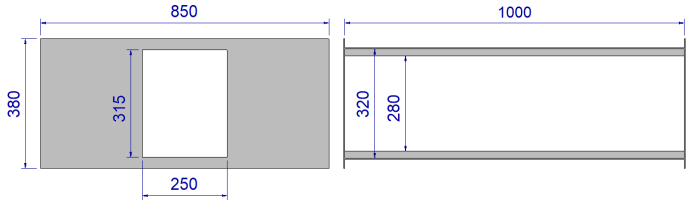

FIG. 2. Principal dimensions of the silencer (in millimetres).

Six types of perforated sheets are evaluated, with systematic variation in both hole geometry and open area ratio. Perforated sheets designated Rv18-26, Qv12-18, and Lv20×5-25×17 are manufactured from 1.5 mm-thick steel sheet, whereas perforated sheets Rv6-12, Rv4-8, and Rv2-3 are manufactured from 1.0 mm-thick steel sheet. Schematic representations of the perforated sheet samples used in the investigation are shown in Fig. 3. The geometric parameters of all tested perforated sheets are summarised in Table 1.

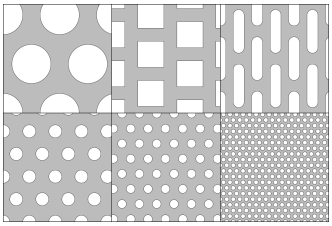

FIG. 3. Schematic views of the perforated sheet samples Rv18-26, Qv12-18, Lv20×5-25×17, Rv6-12, Rv4-8, and Rv2-3 used as side panels in the tested silencer.

TABLE 1. Geometric parameters of the perforated sheets used as inner liners in the absorption silencer.

Designation	Hole shape	Hole size	Pattern	Open area [%]
Rv18-26	Round	18 mm diameter	60° staggered	43.6
Qv12-18	Square	12 mm side		44.0
Lv20×5-25×17	Elongated	20 mm × 5 mm		44.5
Rv6-12	Round	6 mm diameter		22.8
Rv4-8	Round	4 mm diameter		22.8
Rv2-3	Round	2 mm diameter		40.4

For additional comparison, insertion loss measurements are carried out for a configuration comprising only the glass wool, without a perforated sheet.

3. Experiment

3.1. Test rig and operating conditions

The measurements are conducted on a test rig constructed in accordance with ISO 7235 standard (ISO, 2003). The reverberation chamber has a volume of 237.0 m^3 and an area of 231.5 m^2, with non-parallel, sound-reflecting walls. During the measurement of self-noise and pressure drop, the tested silencer is connected to a centrifugal fan via two absorption silencers (Fig. 4). During the measurement of insertion loss, the tested silencer is connected to an external noise source (Fig. 5). The fan, noise source, and tested silencer are positioned outside the reverberation chamber, whereas the outlet is situated inside the chamber. The silencer remains fixed in its position throughout the entire test. Only the upstream source system is reconfigured once, by replacing the fan and its silencers with the loudspeaker source used for the insertion loss measurements. For each perforated-sheet variant, the side panels of the silencer are installed twice: first for the self-noise and pressure-drop measurements, and subsequently for the insertion loss measurements, using the same glass wool slabs in both assemblies.

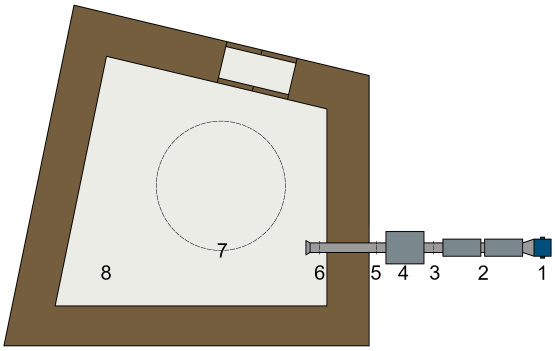

Fig. 4. Test stand with reverberation room scheme for self-noise and pressure drop measurements: 1) fan, 2) set of two silencers, 3) pressure and temperature measurement, 4) test object, 5) pressure measurement, 6) flow velocity measurement, 7) microphone path, 8) reverberation room.

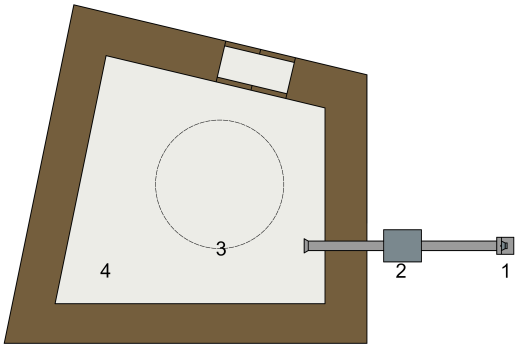

Fig. 5. Test stand with reverberation room scheme for insertion loss measurements: 1) noise source, 2) test object, 3) microphone path, 4) reverberation room.

The airflow rate is controlled by adjusting the frequency of the fan motor using a three-phase inverter, which enables tests at various inlet velocities (4 m/s, 6 m/s, and 8 m/s). The volumetric flow is determined using a Prandtl tube in accordance with ISO 5221 standard (ISO, 1984), with measurements performed in the inlet duct. The static pressure drop across the tested element is measured both upstream and downstream at four circumferentially spaced points using an electronic differential pressure transducer.

3.2. Acoustic and aerodynamic measurements

Acoustic measurements focus on the determination of sound power level in accordance with ISO 3741 standard (ISO, 2010), which specifies precision methods for reverberation chambers. The measuring system comprises a class 1 Norsonic Nor140 sound analyser, a Nor265 rotary table, and the Nor850 software suite. Sound

pressure levels are recorded at twelve points distributed uniformly along a circle with a radius of 1.7 m (circumference 10.7 m) inside the chamber. For each operating condition and each configuration, a single measurement sequence is performed, during which the microphone is successively placed at all twelve positions, while the silencer and duct system remain unchanged. Measurements are performed in 1/3-octave bands within the frequency range from 50 Hz to 10 000 Hz, with each acquisition lasting 30 s.

Background noise is recorded for each measurement series with airflow switched off, enabling calculation of the background correction. Reverberation time is measured for four omnidirectional loudspeaker positions with three microphone positions. All sound power level calculations are completed using a dedicated calculation sheet.

Prior to and following each measurement sequence, instrument calibration is conducted using a class 1 Norsonic Nor1256 calibrator. Additionally, after each measurement set, temperature, relative humidity, and atmospheric pressure are measured and documented, ensuring accurate correction and traceability in the sound power calculation process.

3.3. Statistical analysis

In order to verify whether the differences between the measured values are statistically significant at the 5 % significance level, Student's t-test for two means under the assumption of equal population variances is applied. The statistical procedure follows the approach described in (Montgomery, Runger, 2018). Two independent samples with sizes n_1 and n_2 are considered, for which the sample means $\overline{x_1}$, $\overline{x_2}$, and standard deviations s_1, s_2 are determined. The sample standard deviations are similar in magnitude, which justifies the assumption of homogeneity of variances.

The null hypothesis states that the mean values of the investigated quantity (e.g., insertion loss) under the two measurement conditions are equal:

$$H_0 : \mu_1 = \mu_2, \tag{1}$$

with the alternative hypothesis:

$$H_1 : \mu_1 \neq \mu_2, \tag{2}$$

corresponding to a two-sided test at the significance level $\alpha = 0.05$. In the first step, the pooled estimate of the common variance is computed as

$$s_p^2 = \frac{(n_1 - 1) \cdot s_1^2 + (n_2 - 1) \cdot s_2^2}{n_1 + n_2 - 2}, \tag{3}$$

and the test statistic is then given by

$$t_0 = \frac{\overline{x_1} - \overline{x_2}}{s_p \cdot \sqrt{\frac{1}{n_1} + \frac{1}{n_2}}}. \tag{4}$$

The statistic t_0 follows a Student's t-distribution with $n_1 + n_2 - 2$ degrees of freedom. Based on the calculated value of t_0 and the degrees of freedom $df = n_1 + n_2 - 2$, the p-value is obtained or the critical region determined using the quantile $t_{\alpha/2,df}$. The null hypothesis H_0 is rejected if

$$|t_0| > t_{\alpha/2,df}, \tag{5}$$

which indicates that the difference between the sample means is statistically significant at the 95 % confidence level. Otherwise, there is no statistical evidence to conclude that the mean values differ between the compared silencer configurations.

4. Results

4.1. Insertion loss

Insertion loss is applied to quantify the acoustic performance of the tested silencers. Insertion loss D_i is defined as the reduction in sound power level measured downstream of the silencer resulting from the replacement

of a reference duct section with the silencer under test. In the present study, the reference section is a silencer with glass wool panels covered on the inner side by a solid (non-perforated) metal sheet, whereas the test objects are silencers with glass wool panels covered by a perforated metal sheet or, in one variant, with exposed glass wool. Insertion loss is calculated according to:

$$D_i = L_{WII} - L_{WI}, \tag{6}$$

where L_{WI} is the sound power level in the considered frequency band measured downstream of the silencer with the perforated sheet (or exposed wool), and L_{WII} is the sound power level in the same frequency band measured downstream of the reference silencer with a solid (non-perforated) metal sheet.

This approach enables the evaluation of the acoustic effectiveness associated with the use of perforated sheets of varying aperture size and shape. In addition, a single-number A-weighted insertion loss value is determined for a flat-spectrum noise, assuming a constant sound power level in all frequency bands prior to A-weighting.

Table 2 presents the calculated insertion loss values in octave bands and the single-number A-weighted values for silencers fitted with various internal perforated metal sheets, as well as for the configuration with exposed glass wool. The insertion loss spectra in 1/3-octave bands for all tested configurations are shown in Fig. 6.

Table 2. Insertion loss values in octave bands for silencers with various internal perforated sheets.

f [Hz]	D_i [dB]						
	Rv18-26	Qv12-18	Lv20×5-25×17	Rv6-12	Rv4-8	Rv2-3	Wool itself
63	0.2	−0.1	−0.2	−0.2	−0.5	−0.5	0.0
125	0.9	1.0	0.6	0.6	0.5	0.5	0.8
250	4.2	4.6	4.5	4.9	4.9	4.8	5.0
500	8.5	8.4	8.3	8.4	8.6	8.3	8.3
1000	13.0	13.2	13.4	13.6	13.6	13.3	13.6
2000	6.5	6.6	6.5	8.1	8.2	8.1	8.6
4000	3.5	3.7	3.6	4.7	4.7	4.5	4.7
8000	1.5	1.4	1.4	0.9	0.8	0.8	0.4
A	5.2	5.3	5.2	5.6	5.6	5.5	5.4

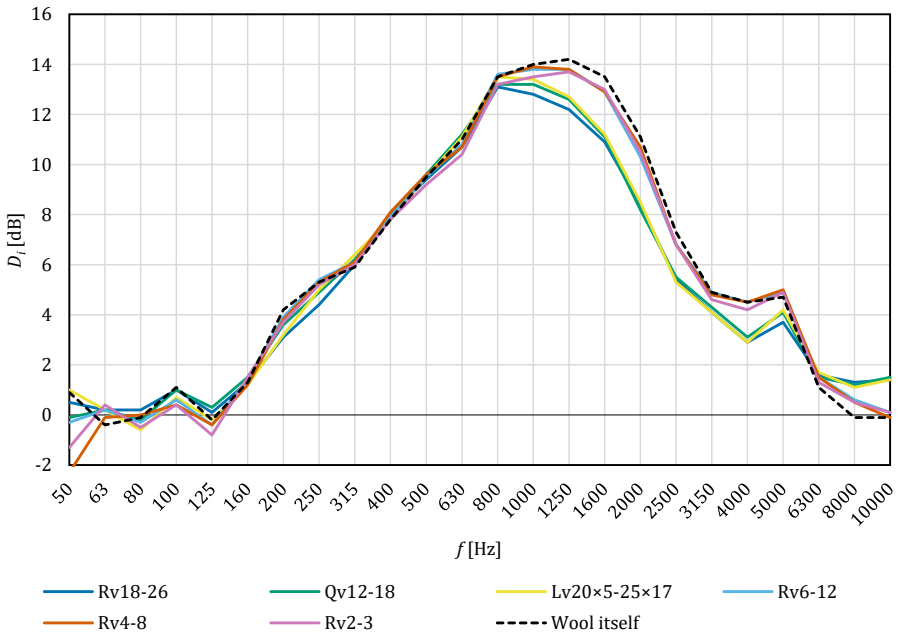

Fig. 6. Insertion loss spectra in 1/3-octave bands for silencers with different internal perforations.

Notable differences are observed between the tested perforated sheets, particularly in the mid- and high-frequency ranges.

In the lowest octave bands (up to 125 Hz), insertion loss is minimal and does not exceed 1 dB for any variant, indicating limited low-frequency attenuation regardless of perforation type. In the range from 250 Hz to 1000 Hz, all configurations achieve similar insertion loss, with values peaking in the 800 Hz to 1250 Hz band.

Above 1000 Hz, the insertion-loss spectra of the individual silencers start to diverge. In the range 1000 Hz to 5000 Hz, silencers with smaller round apertures (Rv6-12, Rv4-8, Rv2-3) generally exhibit higher insertion loss than variants with larger apertures (Rv18-26, Qv12-18, Lv20×5-25×17). At the highest frequencies (above 6300 Hz), the trend reverses, and perforated sheets with larger holes tend to provide higher insertion loss.

To quantify these differences, a two-sample Student's t-test with pooled variance was applied. The analysis shows that the differences between the groups with smaller and larger apertures are statistically significant at the 5 % significance level in the frequency range from 1250 Hz to 2500 Hz and at 4000 Hz and 10 000 Hz, whereas at the remaining frequencies no statistically significant differences between the compared groups are confirmed.

These findings indicate that the type of internal perforated sheet influences insertion loss primarily in the mid- to-high frequency range. Perforated sheets with smaller apertures provide more effective attenuation in those bands where statistically significant differences are observed (mainly from 1250 Hz to 2500 Hz and around 4000 Hz), while at other frequencies the apparent trends in the spectra are not supported by statistical evidence. The shape of the aperture has a secondary effect relative to aperture size.

4.2. Self-noise

Table 3, Table 4, and Table 5 present octave-band sound power levels and overall A-weighted values reported for the self-noise of all tested silencer configurations: perforated sheets, glass wool without an internal sheet, and solid sheet. Each table contains results obtained for a single flow velocity, namely 4 m/s, 6 m/s or 8 m/s. Figure 7 to Fig. 9 illustrate the self-noise spectra in 1/3-octave bands for all tested silencers at flow velocities of 4 m/s, 6 m/s, and 8 m/s, respectively.

Table 3. Sound power levels of self-noise for all silencer configurations (perforated sheets, glass wool, solid sheet): octave-band values and overall A-weighted value at a flow velocity of 4 m/s.

f [Hz]	L_W [dB] at flow velocity 4 m/s							
	Rv18-26	Qv12-18	Lv20×5-25×17	Rv6-12	Rv4-8	Rv2-3	Wool itself	Sheet metal
63	45.0	46.6	45.3	45.3	44.8	45.0	45.0	46.6
125	34.1	34.5	34.1	34.0	34.8	34.7	34.9	35.7
250	34.1	34.5	33.9	33.0	32.7	32.8	32.5	39.7
500	28.3	28.8	28.4	28.0	27.7	27.8	27.7	37.3
1000	18.5	19.1	18.6	17.9	17.7	17.8	17.6	29.5
2000	15.8	16.0	15.9	15.1	15.0	14.9	14.8	21.4
4000	17.3	17.7	17.4	16.8	16.8	16.7	16.7	18.2
8000	20.3	21.1	20.3	20.1	20.1	20.0	20.1	20.5
A	30.2	30.7	30.2	29.6	29.4	29.4	29.3	37.1

Table 4. Sound power levels of self-noise for all silencer configurations (perforated sheets, glass wool, solid sheet): octave-band values and overall A-weighted value at a flow velocity of 6 m/s.

f [Hz]	L_W [dB] at flow velocity 6 m/s							
	Rv18-26	Qv12-18	Lv20×5-25×17	Rv6-12	Rv4-8	Rv2-3	Wool itself	Sheet metal
63	53.2	55.2	53.6	52.9	52.6	52.8	53.1	55.0
125	42.7	42.7	42.7	42.6	42.7	42.7	42.6	44.0
250	42.6	42.7	42.4	41.1	41.2	41.2	40.6	47.6
500	37.4	37.7	37.2	36.9	36.9	36.3	36.1	45.6
1000	31.1	31.5	31.0	30.3	30.2	30.1	29.5	42.2
2000	26.6	27.2	26.8	25.8	25.5	25.2	24.4	37.3
4000	24.6	25.2	24.9	24.1	23.8	23.7	23.2	30.4
8000	21.1	21.9	21.1	20.9	20.9	20.9	20.9	22.2
A	39.1	39.5	39.1	38.3	38.3	38.0	37.6	47.1

TABLE 5. Sound power levels of self-noise for all silencer configurations (perforated sheets, glass wool, solid sheet): octave-band values and overall A-weighted value at a flow velocity of 8 m/s.

f [Hz]	L_W [dB] at flow velocity 8 m/s							
	Rv18-26	Qv12-18	Lv20×5-25×17	Rv6-12	Rv4-8	Rv2-3	Wool itself	Sheet metal
63	58.6	59.5	59.1	57.5	56.9	57.0	57.8	58.7
125	49.0	48.8	49.1	48.5	48.8	48.4	48.6	50.0
250	48.6	48.7	48.4	46.9	47.2	47.0	46.7	53.4
500	43.6	44.0	43.5	42.8	43.0	42.3	42.0	51.2
1000	39.0	39.4	39.0	38.3	38.3	37.6	37.0	49.2
2000	36.5	37.0	36.7	35.7	35.2	35.2	34.3	46.6
4000	34.4	34.9	34.8	33.9	33.6	33.4	33.0	40.9
8000	26.7	27.2	26.9	26.6	26.5	26.4	26.1	30.6
A	46.2	46.5	46.2	45.2	45.3	44.8	44.4	54.1

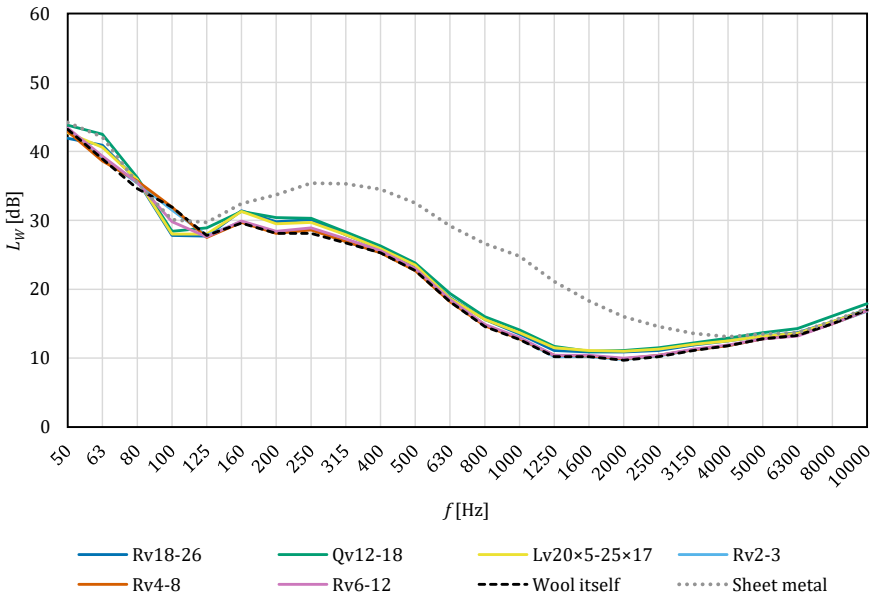

FIG. 7. Self-noise spectra (1/3-octave bands) of silencers at 4 m/s flow velocity.

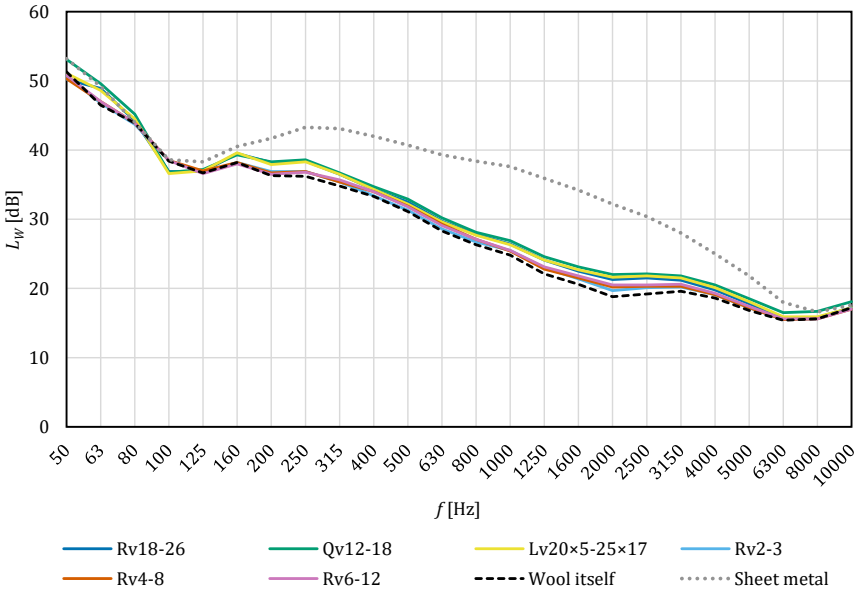

FIG. 8. Self-noise spectra (1/3-octave bands) of silencers at 6 m/s flow velocity.

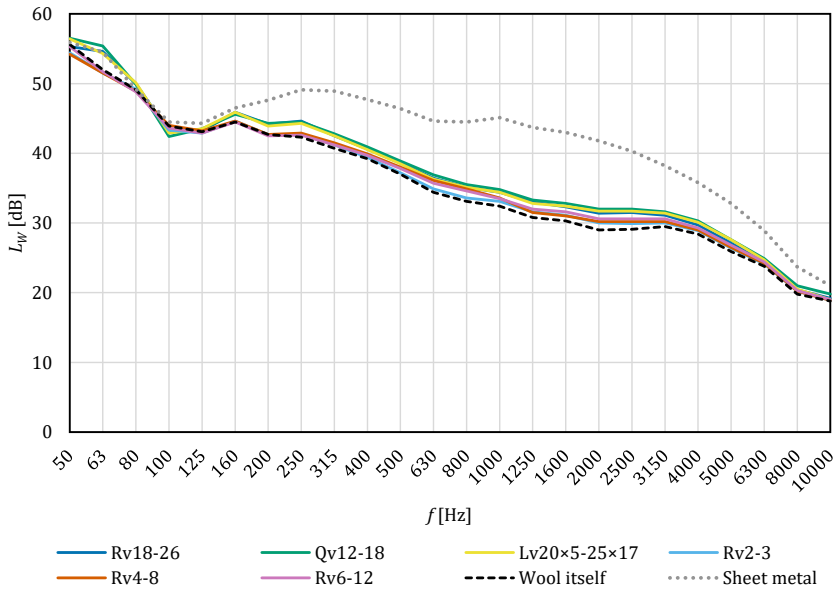

FIG. 9. Self-noise spectra (1/3-octave bands) of silencers at 8 m/s flow velocity.

At a flow velocity of 4 m/s, the self-noise levels of all silencers with perforated sheets are similar and remain within a narrow range. The configuration containing only glass wool exhibits the lowest overall self-noise. In the lowest frequency bands (63 Hz to 250 Hz), differences between perforated sheet variants are negligible, and the levels are close to those observed for this configuration.

To quantify the observed differences between perforated sheet types, a two-sample Student's t-test was applied. For 4 m/s, the analysis indicates that the differences in self-noise between silencers with small apertures (Rv6-12, Rv4-8, Rv2-3) and those with larger or elongated apertures (Rv18-26, Qv12-18, Lv20×5-25×17) are statistically significant at the 5 % significance level in the 160 Hz to 315 Hz and 800 Hz to 4000 Hz bands, whereas at the remaining frequencies no statistically significant differences between these two groups are confirmed.

As the flow velocity increases to 6 m/s and 8 m/s, self-noise levels rise for all configurations. At both higher velocities, silencers with the smallest apertures (Rv6-12, Rv4-8, Rv2-3) generally display lower self-noise values than those with larger or elongated apertures (Rv18-26, Qv12-18, Lv20×5-25×17), particularly in the 500 Hz to 4000 Hz range. For 6 m/s, the t-test shows statistically significant differences between these two groups in the 160 Hz to 315 Hz and 800 Hz to 2500 Hz bands, while for 8 m/s the statistically significant range extends from 160 Hz to 500 Hz and 800 Hz to 2500 Hz. Outside these bands, the apparent differences in the spectra are not confirmed as statistically significant at the 5 % level. The configuration with a solid (non-perforated) inner sheet consistently generates the highest self-noise levels across all velocities, especially in the mid-frequency range, whereas the configuration with exposed wool maintains comparatively low self-noise at all flow rates.

A detailed analysis of the spectral distributions indicates that the largest differences between perforated sheet variants occur in the 160 Hz to 5000 Hz range, particularly at 8 m/s. At the highest flow velocity, silencers with larger apertures tend to exhibit increased self-noise in this range compared to those with small apertures.

In summary, the type of perforation in the internal sheet of the silencer has a measurable influence on self-noise, especially at elevated flow velocities and in the 160 Hz to 5000 Hz range. Perforated sheets with smaller apertures provide a moderate reduction in self-noise relative to variants with larger or elongated apertures in those bands where statistically significant differences are observed, while a solid sheet as the inner lining results in unfavourable self-noise performance over most of the spectrum.

4.3. Pressure loss

Table 6 presents the measured pressure loss values for the silencer with various internal perforated sheets, as well as for the configurations with exposed glass wool and a solid (non-perforated) sheet, at flow velocities of

Table 6. Pressure loss of silencers with various perforated sheets at different flow velocities.

v [m/s]	Δp [Pa]							
	Rv18-26	Qv12-18	Lv20×5-25×17	Rv6-12	Rv4-8	Rv2-3	Wool itself	Sheet metal
4	1.8	1.8	1.9	1.8	2.0	1.4	1.6	2.1
6	4.0	4.3	3.9	3.8	4.2	3.5	3.8	4.2
8	6.8	7.1	6.3	6.3	7.0	6.2	6.6	7.0

4 m/s, 6 m/s, and 8 m/s. Figure 10 shows the average pressure loss as a function of flow velocity for all tested configurations.

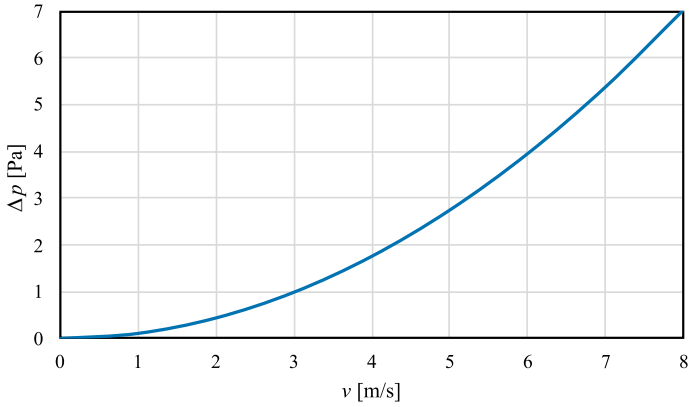

Fig. 10. Average pressure loss of silencers as a function of flow velocity.

The pressure losses observed for all variants increase with flow velocity and remain consistent across different types of internal perforated sheets. For each flow velocity, the differences between configurations do not exceed 1 Pa. Both the configuration with exposed glass wool and that with a solid sheet exhibit pressure losses within the same range as the perforated sheet variants.

These results indicate that the type and geometry of the internal perforated sheet have a negligible effect on the overall pressure loss of the silencer, and the pressure loss characteristics are primarily governed by the total flow resistance of the silencer assembly.

5. Conclusions

This paper investigated the impact of perforated sheet metal on the performance of absorptive silencers, focusing on insertion loss, self-noise, and pressure loss characteristics. The study utilised a modular silencer test rig with replaceable side panels, allowing for the evaluation of various perforated sheet geometries (circular, square, elongated), sizes and perforation ratios. Glass wool (Ventilux 6335, 100 mm thick) served as the sound-absorbing material. Insertion loss measurements were conducted in a reverberation chamber according to ISO 7235 (ISO, 2003), across the 50 Hz to 10 000 Hz frequency range. The same glass wool layers were used in all measurements, ensuring constant properties of the absorption material throughout the test. Furthermore, acoustics measurements were based on averaging over 12 different microphone positions in the reverberation chamber. All acoustic measurements were performed using the same measurement instrumentation.

Insertion loss tests revealed that all silencer variants exhibited minimal attenuation at low frequencies (below 160 Hz). In the 250 Hz to 1000 Hz range, all perforated sheet variants and the wool-only configuration achieved similar, relatively high insertion loss values, with a maximum around 1000 Hz. Above 1000 Hz, silencers with smaller round apertures (Rv6-12, Rv4-8, Rv2-3) provided higher insertion loss in the 1000 Hz to 5000 Hz range, whereas for frequencies above 6300 Hz, perforated sheets with larger apertures (Rv18-26, Qv12-18, Lv20×5-25×17) offered superior attenuation. The statistical analysis based on two-sample Student's t-test with pooled variance confirmed that the differences in insertion loss between the group with larger or elongated apertures (Rv18-26,

Qv12-18, Lv20×5-25×17) and the group with smaller round apertures (Rv6-12, Rv4-8, Rv2-3) are statistically significant at the 5 % significance level in the 1250 Hz to 2500 Hz bands, as well as at 4000 Hz and 10 000 Hz, while at the remaining frequencies the observed differences were not confirmed as statistically significant.

Self-noise measurements showed that, at a flow velocity of 4 m/s, all tested configurations exhibited similar levels, with the wool-only configuration having the lowest overall self-noise. As the flow velocity increased to 6 m/s and 8 m/s, self-noise levels rise for all silencers and the differences between perforated sheet types became more apparent: silencers with the smallest apertures (Rv6-12, Rv4-8, Rv2-3) consistently exhibited slightly lower self-noise, particularly in the 160 Hz to 5000 Hz range. Silencers equipped with a solid (non-perforated) inner sheet generated the highest self-noise levels across all test conditions, especially in the mid-frequency bands. For all investigated flow velocities, the statistical evaluation indicated that the differences in self-noise between silencers with small round apertures and those with larger or elongated apertures were statistically significant in the 160 Hz to 315 Hz and 800 Hz to 2500 Hz bands, whereas outside these ranges the apparent differences in the spectra were not confirmed as statistically significant at the 5 % level.

Pressure loss measurements demonstrated that, for all tested variants, pressure loss increased proportionally with airflow velocity and remained consistent between different perforated sheet types. The differences in pressure drop for a given velocity did not exceed 1 Pa, and the absolute values were similar for perforated, solid, and wool-only configurations. Thus, the geometry of the internal perforated sheet had a negligible effect on pressure loss in this silencer type.

A key observation is that the Rv18-26 and Rv2-3 perforated sheets had identical aperture shape (round) and a similar perforation ratio (43.6 % for Rv18-26 and 40.4 % for Rv2-3), yet their performance differed significantly. The Rv2-3 sheet, with smaller holes, provided much higher insertion loss and lower self-noise in the mid-frequency range compared to Rv18-26, which had much larger apertures. Therefore, it can be concluded that it is primarily the aperture size (not the shape or perforation ratio) that governs acoustic effectiveness in absorptive silencers. This conclusion is supported by the statistical results, which systematically demonstrate significant differences between the groups with small and large apertures in the mid-frequency range for both insertion loss and self-noise. It should be noted that the perforated sheets with smaller apertures (Rv6-12, Rv4-8, Rv2-3) had a thickness of 1.0 mm, whereas the sheets with larger apertures (Rv18-26, Qv12-18, Lv20×5-25×17) were 1.5 mm thick, which may also influence the silencer performance. Although the small- and large-aperture sheets also differed in thickness (1.0 mm vs 1.5 mm), the comparison of Rv2-3 and Rv18-26 (similar open area ratio and identical hole shape) indicates that the aperture diameter is the dominant factor affecting insertion loss.

The results demonstrate that perforated sheets with small round apertures (Rv6-12, Rv4-8, Rv2-3) ensure the most favourable combination of high insertion loss across a wide frequency range and low self-noise, without causing any measurable increase in pressure loss. These findings suggest that, for ventilation and noise control applications, the use of perforated sheets with small circular apertures enables effective noise reduction without compromising airflow performance. In the acoustic measurements, the same test silencer remained in place. The only change in the setup was the sound source, which was switched once from the fan unit with silencers to a loudspeaker system for insertion loss determination. For each perforated configuration, the side panels were mounted twice: once for self-noise and pressure loss measurements, and once for insertion loss measurements after switching the sound source. In both types of acoustic tests (insertion loss and self-noise), panels with smaller perforation (Rv6-12, Rv4-8, Rv2-3) consistently exhibited superior acoustic performance compared to panels with larger apertures.

Fundings

This research did not receive any specific grant from funding agencies in the public, commercial, or not-for-profit sectors.

Conflict of interests

The authors declare that they have no known competing financial interests or personal relationships that could have appeared to influence the work reported in this paper.

Authors' contributions

Kamil Wójciak performed the measurements, analysed and interpreted the data, and wrote the original draft. Joanna Maria Kopania conceptualized the study and contributed to the analysis and interpretation of the data. Patryk Gaj performed the measurements and contributed to the analysis and interpretation of the data. All authors reviewed and approved the final manuscript.

References

1. Abramkina D. (2023), Noise from mechanical ventilation systems in residential buildings, *E3S Web of Conferences*, **457**: 02007, https://doi.org/10.1051/e3sconf/202345702007.
2. Allam S., Łbom M. (2011), A new type of muffler based on microperforated tubes, *Journal of Vibration and Acoustics*, **133**(3): 031005, https://doi.org/10.1115/1.4002956.
3. Asdrubali F., Pispola G. (2007), Properties of transparent sound-absorbing panels for use in noise barriers, *The Journal of the Acoustical Society of America*, **121**(1): 214–221, https://doi.org/10.1121/1.2395916.
4. Gaj P., Kopania J., Wójciak K., Bogusławski G. (2019), Assessment of sound absorbing properties of composite made of recycling materials, *Vibrations in Physical Systems*, **30**(1): 2019109.
5. Harvie-Clark J., Conlan N., Wei W., Siddall M. (2019), How loud is too loud? noise from domestic mechanical ventilation systems, *International Journal of Ventilation*, **18**(4): 303–312, https://doi.org/10.1080/14733315.2019.1615217.
6. Hoshi K. *et al.* (2020), Implementation experiment of a honeycomb-backed MPP sound absorber in a meeting room, *Applied Acoustics*, **157**: 107000, https://doi.org/10.1016/j.apacoust.2019.107000.
7. International Organization for Standardization (1984), *Air distribution and air diffusion – Rules to methods of measuring air flow rate in an air handling duct* (ISO Standard No. 5221:1984), https://www.iso.org/standard/11223.html.
8. International Organization for Standardization (2003), *Acoustics – Laboratory measurement procedures for ducted silencers and air-terminal units – Insertion loss, flow noise and total pressure loss* (ISO Standard No. 7235:2003), https://www.iso.org/standard/30385.html.
9. International Organization for Standardization (2010), *Acoustics – Determination of sound power levels and sound energy levels of noise sources using sound pressure – Precision methods for reverberation test rooms* (ISO Standard No. 3741:2010), https://www.iso.org/standard/52053.html.
10. Kang J., Brocklesby M.W. (2005), Feasibility of applying micro-perforated absorbers in acoustic window systems, *Applied Acoustics*, **66**(6): 669–689, https://doi.org/10.1016/j.apacoust.2004.06.011.
11. Lan L., Sun Y., Wyon D.P., Wargocki P. (2021), Pilot study of the effects of ventilation and ventilation noise on sleep quality in the young and elderly, *Indoor Air*, **31**(6): 2226–2238, https://doi.org/10.1111/ina.12861.
12. Maa D.-Y. (1998), Potential of microperforated panel absorber, *The Journal of the Acoustical Society of America*, **104**(5): 2861–2866, https://doi.org/10.1121/1.423870.
13. Montgomery D.C., Runger G.C. (2018), *Applied Statistics and Probability for Engineers*, Wiley, Hoboken.
14. Wu M.Q. (1997), Micro-perforated panels for duct silencing, *Noise Control Engineering Journal*, **45**(2): 69–77, https://doi.org/10.3397/1.2828428.
15. Wójciak K., Kopania J.M., Gaj P. (2025), Acoustic properties of the absorption silencers with a micro-perforated channel in the air-flow, *Vibrations in Physical Systems*, **36**(1): 2025112, https://doi.org/10.21008/j.0860-6897.2025.1.12.
16. Yang C., Cheng L. (2016), Sound absorption of microperforated panels inside compact acoustic enclosures, *Journal of Sound and Vibration*, **360**: 140–155, https://doi.org/10.1016/j.jsv.2015.09.024.
17. Yang C., Cheng L., Hu Z. (2015), Reducing interior noise in a cylinder using micro-perforated panels, *Applied Acoustics*, **95**: 50–56, https://doi.org/10.1016/j.apacoust.2015.02.003.
18. Yu X., Cui F.S., Cheng L. (2016), On the acoustic analysis and optimization of ducted ventilation systems using a sub-structuring approach, *The Journal of the Acoustical Society of America*, **139**(1): 279–289, https://doi.org/10.1121/1.4939785.
19. Zhang X., Yang C., Cheng L., Zhang P. (2020), An experimental investigation on the acoustic properties of micro-perforated panels in a grazing flow, *Applied Acoustics*, **159**: 107119, https://doi.org/10.1016/j.apacoust.2019.107119.